Transaction B: Mechanical Engineering
Vol. 17, No. 2, pp. 121–135

SCIENTIA IRANICA

Maximum Dynamic Load Determination of Mobile Manipulators via Nonlinear Optimal Feedback

H. Korayem[1,*] **and M. Irani**[1]

Abstract. *In this paper, a nonlinear optimal feedback control law is designed to find the maximum load carrying capacity of mobile manipulators for a given trajectory task. The optimal state feedback law is given by the solution to the nonlinear Hamilton-Jacobi-Bellman (HJB) equation. An iterative procedure is used to find a sequence of approximate solutions of the HJB equation. This is done by solving a sequence of Generalized HJB (GHJB) differential equations. The Galerkin procedure is applied to find a numerical solution to the GHJB equation. Using this method, a nonlinear feedback is designed for the mobile manipulator and, then, an algorithm is developed to find the maximum payload. In mobile base manipulators, the maximum allowable load is limited by their joint actuator capacity constraints, nonholonomic constraints and redundancy that arise from base mobility and increased Dofs. To solve the extra Dofs of the system, an extended Jacobian matrix and additional kinematic constraints are used. The validity of the methodology is demonstrated via simulation for a two-link wheeled mobile manipulator and linear tracked Puma arm and the results are discussed.*

Keywords: *Maximum payload; Manipulator; Optimal control; Closed loop controller; HJB.*

INTRODUCTION

Mobile manipulators have a compact structure, large workspace and high maneuverability and are cost effective. One of the main usages of mobile manipulators is handling loads on a given trajectory. Therefore, to maximize the productivity and economic usage of these manipulators, finding the maximum allowable load is necessary. The Dynamic Load Carrying Capacity (DLCC) of a manipulator for a given end-effecter trajectory is defined as the maximum load that the manipulator can carry on the defined trajectory with sufficient accuracy. Wang and Ravani [1] formulated DLCC as an optimization problem using state space representation of the dynamic equation of motion. Wang et al. [2] developed a point-to-point motion planner for open-chained robots. The optimal control problem is converted into a direct SQP parameter optimization in which the gradient is determined analytically and, then, the algorithm has been applied to a Puma 762 robot. Korayem et al. solved the problem of finding the maximum load carrying capacity of a mobile manipulator as a trajectory optimization problem [3]. The dynamic equation of motion is linearized and iterative linear programming is used to solve the optimization problem.

The maximum allowable load of mobile manipulators is limited by their joint actuator capacity constraints, the trajectory tracking accuracy, redundancy and nonholonomic constraints, where redundancy and nonholonomic constraints are arisen from base mobility and increased Dofs. A unique solution for the maximum allowable load is not feasible. The solution for the maximum allowable load depends on the type of user-defined constraints to the redundancy resolution. Korayem and Gariblu [4] found the maximum allowable load of a redundant mobile manipulator via two different additional functions that are applied to resolve the motion redundancy. Xu et al. [5] investigated motion planning for a mobile manipulator with redundant Dofs

1. *Robotic Research Laboratory, College of Mechanical Engineering, Iran University of Science and Technology, Tehran, P.O. Box 18846, Iran.*
*. *Corresponding author. E-mail: hkorayem@iust.ac.ir*

Received 7 May 2009; received in revised form 10 August 2009; accepted 10 November 2009

to track a desired trajectory. Korayem et al. [6,7] used the open loop optimal control approach to find the DLCC of fixed and redundant mobile manipulators. Pontryagin's minimum principle is used to derive optimality conditions and the problem is improved to the Two Point Boundary Value Problem (TPBVP) that is solvable with MATLAB software. In the case of mobile manipulators, nonholonomic constraints and redundancy complicate the problem. The extended Jacobian matrix and additional kinematic constraints are used to solve the extra Dofs of the manipulator. In [8], Kelly and Nagy have addressed a method to find optimal paths by formulating an optimal control problem and solving the nonlinear programming problem via the Lagrange method. Furuno et al. [9] solved the trajectory planning problem of a mobile manipulator. A zero moment point criterion is used as a stability index. The problem is formulated as an optimal control problem and a hierarchical gradient method is used to solve it. In [10], a new methodology to perform the optimal path planning of robot manipulators in the presence of moving obstacles was presented. An algorithm is proposed for finding the maximum load carrying capacity of a flexible parallel robot for a given trajectory in [11].

The solutions in these researches are open loop and are generally not useful for practical applications. Willigenburg et al. [12] applied open loop optimal control together with linear optimal feedback. Firstly, the optimization problem is solved via the open loop optimal control approach, optimal inputs and states are determined and, then, an approximate model that is linearized about the optimal state and control trajectories is used to design the linear optimal feedback. A model-based controller is designed for the mobile manipulator to follow the desired end-effector trajectory without violating nonholonomic constraints in [13]. Song et al. [14] designed a model-based tracking controller in the presence of dynamical uncertainties and obtained a globally asymptotic stability in a Lyapunov sense. Reyes and Rosado [15] have introduced the polynomial family of PD-type controllers as an algorithm for position control of robot manipulators. The performance of the scheme was compared with other algorithms, such as PD and PID controllers.

With the existence of uncertainties and disturbances, robust methodologies can be used to design control systems. Mailah et al. [16] used a resolved acceleration control to manipulate the kinematic component and implemented a proportional integral active force control to compensate the dynamic effects, including the bounded disturbances and uncertainties, for a mobile manipulator to track a prescribed trajectory. Tae Jun Ha et al. [17] proposed a robust inverse-optimal control for flexible joint robot manipulators.

Abdessemed [18] et al. used a robust fuzzy-based controller for tracking the trajectory task of mobile manipulators. The dynamic model of the manipulator and the kinematic model of the mobile base are used in simulations. Tran et al. [19] applied a sliding mode control method for a two-wheel welding mobile manipulator to track a smooth curved welding path. A sliding surface is set up and a control law, based on Lyapunov stability, is designed for stabilizing the sliding surface.

Using closed loop controllers, the DLCC of a mobile manipulator can be determined and the results will be more applicable than using an open loop computation. The DLCC of a flexible two link mobile manipulator is calculated in [20]. Finite element and feedback linearization methods are used for modeling and control, respectively. Korayem et al. [21] proposed an algorithm to improve the maximum load carrying capacity of flexible manipulators in the presence of a closed loop controller. The designed controller is divided into two steps: partial feedback linearization and sliding mode approach and, then, a state observer is designed for measuring the velocity of elastic variables.

Because finding DLCC is an optimization problem, it is appropriate to apply an optimal feedback controller to reduce the amount of torque in joints and increase tracking accuracy. If manipulators carry a specified load via less torque in the joints, the DLCC of the manipulator will be increased. Some papers focus on using optimal feedback for manipulators. Green and Sasiadek [22] presented three different methods for the endpoint tracking task of a manipulator using inverse dynamic, linear quadratic regulator and fuzzy logic schemes. In [23], a performance functional-based controller is designed for a redundant mobile manipulator in the task space of the end-effector. An optimal state feedback control scheme is developed for motion control of a manipulator with redundant joints and a linearized model of the dynamics of the manipulator is used in control algorithm. In all these articles, approximate linear equations of motion of a manipulator are used but, in this paper, a nonlinear optimal feedback control law is designed for a mobile manipulator.

Optimal control of nonlinear systems is one of the most active subjects in control theory. The main difficulty with optimal control theory is that, in order to determine optimal control for a nonlinear system, the Hamilton-Jacobi-Bellman (HJB) Partial Differential Equation (PDE) has to be solved [24]. There is rarely an analytical solution to this equation, although several numerical computation approaches have been proposed to obtain the approximate solution to the HJB equation for general nonlinear dynamical models. Beeler et al. [25] carried out a comprehensive comparison study of five methods for the synthesis of nonlinear optimal control systems and the performance of each method is studied on several test problems. An optimal predictive control approach [26], a power series solution [27] and the SDRE (State-Dependent Riccati Equation) control that is an extension of the Riccati equation to nonlinear systems [28,29] are other examples to the solution of the nonlinear optimal control problem. A solution method with a closed-loop result is combining successive approximation and Galerkin approximation in [30]. The procedure is broken into two parts. At first, the HJB equation is reduced to an infinite sequence of differential equations named Generalized Hamilton-Jacobi-Bellman (GHJB) equations. Then, Galerkin's method is used to approximate the GHJB equation. Combining these two methods produces a closed-loop stabilizing control law on a well-defined region of state space.

In this paper, determining the maximum allowable load of mobile manipulators for a given end-effector trajectory is solved by using the nonlinear optimal feedback controller. The extra Dofs are solved using the additional constraint functions and the augmented Jacobian matrix. Using the successive approximation method, nonlinear optimal feedback is designed. Then, an algorithm for determining the maximum payload on a given trajectory is proposed. In order to verify the proposed method, simulations are performed for a two-link planar manipulator mounted on a differentially driven mobile base and a linear tracked Puma arm.

KINEMATIC AND DYNAMIC MODELING

Kinematic Modeling and Redundancy Resolution

Assume that q is the generalized coordinates of the system:

$$q = [q_1, \cdots, q_{n_s}] = [q_b, q_m]. \tag{1}$$

If n_b is the number of mobile base Dofs and n_m is the number of manipulator Dofs, then the overall system degrees of freedom will be $n_s = n_b + n_m$. Consider that the position of the end-effector has m degrees of freedom in Cartesian space and determined as:

$$X = X(q) = [x_e, y_e, z_e]^T. \tag{2}$$

The kinematic relation between the end-effector velocity and the rate of generalized coordinates can be determined as:

$$\dot{X} = J\dot{q} = [J_b, J_m][\dot{q}_b, \dot{q}_m]^T. \tag{3}$$

In this equation, $\dot{X} \in R^{n_e}$ denotes the end-effector velocity and $\dot{q} \in R^{n_s}$ is the joints velocity vector. Because often $n_s > n_e$, the mobile manipulator system is kinematically redundant and extra degrees of freedom on its motion is equal to $R = n_s - n_e$. For redundancy resolution, an extended Jacobian matrix concept is used [6]. In this method, additional suitable kinematic constraints are applied to system dynamics. The motion of the mobile manipulator may be limited by the number of either holonomic or nonholonomic constraints. Consider c to be the number of nonholonomic constraints and the generalized form of these constraint equations will be:

$$J_c\dot{q} = 0. \tag{4}$$

$J_c \in R^{c\times n_s}$ is the matrix of the corresponding coefficients of the time derivative of motion variables in the nonholonomic constraints. For redundancy resolution, R extra degrees of freedom must be solved. Using c nonholonomic constraints, r additional functions must be applied to relate joint vectors where $r = R - c$. Because of this, we apply r extra holonomic constraints in general form, $X_z = Z(q)$. The time derivative of this equation is:

$$\dot{X}_z = J_z\dot{q}, \tag{5}$$

where $J_z \in R^{r\times n_s}$ is the matrix of the corresponding coefficients of time derivative of generalized coordinates in $Z(q)$. Combining Equations 3 to 5, the kinematic equation of mobile manipulators becomes:

$$\begin{bmatrix}\dot{X} & \dot{X}_z & 0\end{bmatrix}^T = \begin{bmatrix}J & J_z & J_c\end{bmatrix}^T \dot{q} = J_a\dot{q}. \tag{6}$$

The augmented Jacobian matrix, J_a, must be non-singular. So, r additional holonomic constraints must be selected properly. Using Equation 6, the velocity and acceleration of vector q can be determined as:

$$\dot{q} = J_a^{-1}\begin{bmatrix}\dot{X} & \dot{X}_z & 0\end{bmatrix}^T, \tag{7}$$

$$\ddot{q} = J_a^{-1}\left(\begin{bmatrix}\ddot{X} & \ddot{X}_z & 0\end{bmatrix}^T - \dot{J}_a\dot{q}\right). \tag{8}$$

Dynamic Modeling and State Space Representation

For a mobile manipulator with generalized coordinates as Equation 1 and an input vector (forces and torques) such as $U = [u_1, \cdots, u_n]$, the dynamic model can be written as:

$$U = M(q)\ddot{q} + C(q, \dot{q}) + G(q), \tag{9}$$

where $M \in R^{n_s\times n_s}$ and C, $G \in R^{n_s}$. If a number of n_e coordinates describe a task trajectory in task space and $n_s > n_e$, then generalized coordinate vector q can be separated as:

$$q = \begin{bmatrix}q_r & q_{nr}\end{bmatrix}^T, \tag{10}$$

where $q_r \in R^{r+c}$ contains generalized coordinates determined directly by applying r holonomic constraints and c nonholonomic constraints to the system. The remaining non-redundant generalized coordinates are in the vector $q_{nr} \in R^{n_e}$. These n_e non-redundant Dofs accomplish the desired task. In a similar way, dynamic Equation 9 can be decomposed into two parts: One corresponds to a redundant and another to a non-redundant set of variables [6]:

$$\begin{bmatrix} U_r \\ U_{nr} \end{bmatrix} = \begin{bmatrix} M_{r,r} & M_{r,nr} \\ M_{r,nr} & M_{nr,nr} \end{bmatrix} \begin{bmatrix} \ddot{q}_r \\ \ddot{q}_{nr} \end{bmatrix} + \begin{bmatrix} C_r + G_r \\ C_{nr} + G_{nr} \end{bmatrix}. \tag{11}$$

Redundant variables and their derivatives q_r, $\dot{q}_r$ and $\ddot{q}_r$ are determined according to the redundancy resolution, thus $M_{r,nr}$, $M_{nr,nr}$ and G_{nr} will be appeared as functions of time and q_{nr}. Also, C_{nr} is a functions of time, q_{nr} and $\dot{q}_{nr}$. So, the second row of Equation 11 describes the dynamic of the non-redundant part of the system and is in the form:

$$U_{nr} = M_{nr,nr}\ddot{q}_{nr} + (M_{r,nr}\ddot{q}_r + C_{nr} + G_{nr}). \tag{12}$$

In this second order differential equation, the only variables are time and q_{nr} and by defining state space variables as:

$$x = \begin{bmatrix} x_1 & x_2 \end{bmatrix}^T = \begin{bmatrix} q_{nr} & \dot{q}_{nr} \end{bmatrix}^T. \tag{13}$$

The state space representation of system can be formulated as:

$$\dot{x} = \begin{bmatrix} \dot{x}_1 & \dot{x}_2 \end{bmatrix}^T = \begin{bmatrix} x_2 & N(x) + Z(x)U \end{bmatrix}, \tag{14}$$

where $N \in R^{n_e}$ and $Z \in R^{n_e \times n_e}$ are:

$$N = -M_{nr,nr}^{-1}(M_{r,nr}\ddot{q}_r + C_{nr} + G_{nr}),$$

$$Z = M_{nr,nr}^{-1}. \tag{15}$$

STRUCTURE OF NONLINEAR OPTIMAL CONTROLLER

Optimal Control and HJB Equation

Consider a nonlinear system of the form:

$$\dot{x} = f(x) + g(x)u(x), \tag{16}$$

and a scalar cost function:

$$J(x) = \int_0^\infty (x^TQx + u^T(x)\mathrm{R}u(x))dt, \tag{17}$$

where $x \in R^n$ and $u \in R^m$. Q is a constant $n \times n$ symmetric positive semi-definite matrix and R is a $m \times m$ symmetric positive definite matrix. The optimal control problem is to find a state feedback control, $u(x)$, which minimizes the cost function, $J(x)$. For a linear system with linear f and g, the optimal control must be found through solving the Riccati equation. But, for a nonlinear system described with Equation 16, according to the calculus of variations, the optimal solution is found through solving the Hamilton-Jacobi-Bellman (HJB) partial differential equation [25]:

$$J_x^{*T}(f + gu^*) + x^TQx + u^{*T}\mathrm{R}u^* = 0, \tag{18}$$

and the optimal control law determined from:

$$u^* = -\frac{1}{2}R^{-1}g^TJ_x^*. \tag{19}$$

The HJB equation is very difficult to solve analytically and must be solved numerically.

Iterative Solution

The main idea of an iterative solution is to solve Equations 18 and 19 together with an iterative process [25]. Suppose $u^{(0)}(x)$ is an initial control law with the stability region Ω, then, the solution of the HJB equation can be found using an iterative algorithm as shown in Figure 1. In this algorithm, ε is desired accuracy and u_ε^* is the final approximation of u^*. The equation:

$$\frac{\partial J^T}{\partial x}(f + gu) + x^TQx + u^T\mathrm{R}u = 0, \tag{20}$$

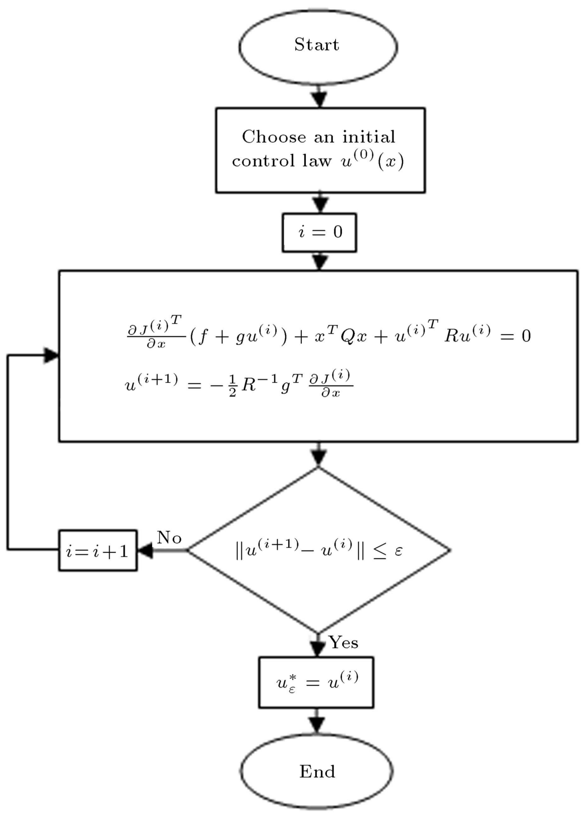

Figure 1. Successive approximation algorithm.

is solved in any iteration of the successive approximation algorithm and is named the Generalized HJB equation (GHJB) where u is a known function of x. The GHJB equation is difficult to solve analytically. So, the Galerkin method is used for the numerical solution of this equation.

Numerical Solution to the GHJB Equation

In the Galerkin method, a set of N suitable basis functions, $\{\phi_j(x)\}_{j=1}^N$, is selected and also it is supposed that a finite approximate solution to the GHJB equation will be of the form:

$$J_N(x) = \sum_{j=1}^{N} c_j \phi_j(x). \tag{21}$$

According to the Galerkin method, the coefficients, c_j, are determined by solving the set of N algebraic equations as below [26]:

$$\int_\Omega \left(\frac{\partial J_N(x)}{\partial x}(f+gu) + x^T Q x + u^T \mathrm{Ru} \right) .\phi_j(x)dx = 0,$$

$$j = 1, \cdots, N. \tag{22}$$

If we use the notation $C_N = [c_1, \cdots, c_N]^T$ and $\Phi_N = [\phi_1, \cdots, \phi_N]^T$, then, Equation 22 can be rewritten as:

$$(A_f + A_u)C_N = B_Q + B_u, \tag{23}$$

where:

$$A_f = \int_\Omega \Phi_N f^T \nabla \Phi_N^T dx, \tag{24}$$

$$A_u = \int_\Omega \Phi_N u^T g^T \nabla \Phi_N^T dx, \tag{25}$$

$$B_Q = \int_\Omega x^T Q x \Phi_N dx, \tag{26}$$

$$B_u = -\int_\Omega \Phi_N u^T R^{-1} u_d x. \tag{27}$$

Note that in Equation 22, if u is a known function of x, as the form:

$$u_N(x) = -\frac{1}{2} R^{-1} g^T \frac{\partial J_N(x)}{\partial x} = -\frac{1}{2} R^{-1} g^T \nabla \Phi^T c_N, \tag{28}$$

then, A_u and B_u can be calculated as $A_u = -\frac{1}{2}\sum_{j=1}^{N} c_j G_j$ and $B_u = -\frac{1}{4}\sum_{j=1}^{N} c_j G_j C_N$ that G_j is:

$$G_j = \int_\Omega \Phi_N \frac{\partial \phi_j^T}{\partial x} g R^{-1} g^T \nabla \Phi_N^T dx. \tag{29}$$

So, if $A = A_f + A_u$ and $B = B_Q + B_u$, then vector C_N will be computed as follows:

$$C_N = A^{-1} B. \tag{30}$$

Now, the successive approximation algorithm and the Galerkin method can be combined to derive a new algorithm for computing a sequence of coefficients vector, $C_N^{(j)} = [c_1^{(j)}, \cdots, c_N^{(j)}]^T$, and to find $u_\delta^*(x)$ that is an approximate value of $u_\varepsilon^*(x)$. The algorithm is applied until $C_j^{(i)}$ and $C_j^{(i+1)}$ are closed to each other with δ accuracy as shown in Figure 2.

NEW ALGORITHM FOR MAXIMUM PAYLOAD CALCULATION

The DLCC of a manipulator for a given end-effecter trajectory is defined as the maximum load that the

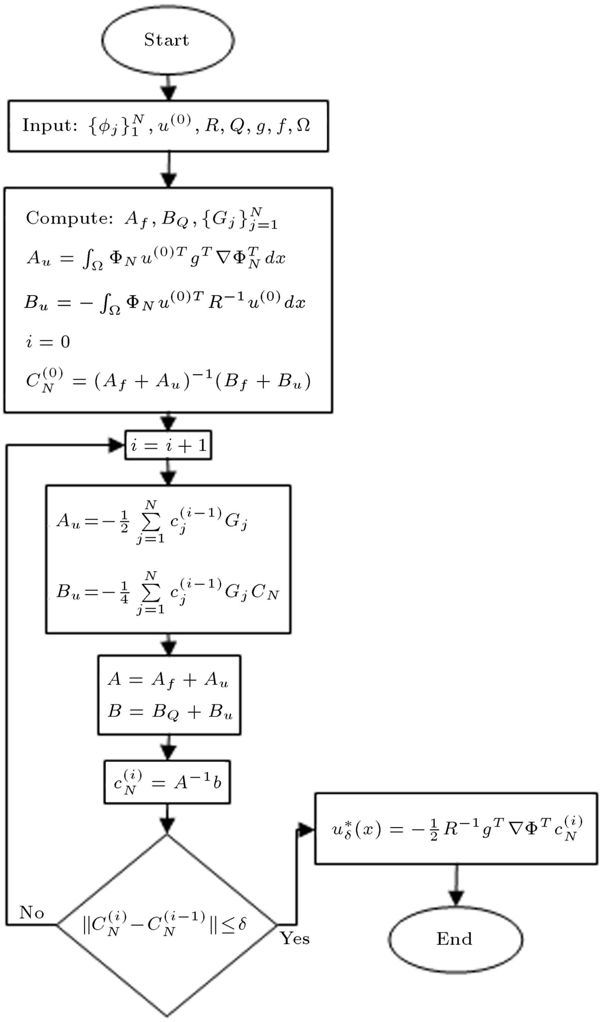

Figure 2. Algorithm for numerical solution to the GHJB equation.

manipulator can carry on the defined trajectory with sufficient accuracy. Excessive deviations from the given trajectory at the end-effector could be attributed to manipulator and load inertia, the dynamic effects of a closed-loop controller and the dynamic interactions between the mobile base and manipulator. The amplitude of this deviation must be bounded for an allowable tracking task. The position of the end-effector, $X(q(t))$, at each time is calculated by Equation 2. If the tracking accuracy is α and desired trajectory is $X_d(q(t))$, then the accuracy constraint will be as follows:

$$\|X_d(q(t)) - X(q(t))\| \leq \alpha. \tag{31}$$

The other main constraint which bounds the DLCC of the mobile manipulator is the limitation of the torque in actuators. The joint actuator torque constraint is formulated based on the typical torque-speed characteristics of DC motors. The upper and lower value of the allowable torque of each joint can be calculated as:

$$\tau_{i\max} = \tau_s - \frac{\tau_s}{\omega_{nl}}\dot{q}_i,$$

$$\tau_{i\min} = -\tau_s - \frac{\tau_s}{\omega_{nl}}\dot{q}_i. \tag{32}$$

The value of each joint torque can be determined as:

$$\tau_i = \begin{cases} \tau_{i\max} & \text{if } u_i > \tau_{i\max} \\ u_i & \text{if } \tau_{i\min} \leq u_i \leq \tau_{i\max} \\ \tau_{i\min} & \text{if } u_i < \tau_{i\min} \end{cases} \tag{33}$$

u_i is calculated using Equation 19.

Using algorithms shown in Figures 1 and 2, a nonlinear optimal controller is designed for the mobile manipulator and, then the DLCC of the manipulator is determined using a new algorithm as shown in Figure 3. This algorithm has three main parts. In the first part, the proper trajectory is selected and holonomic and nonholonomic constraints are added. Then, the redundancy resolution is applied to find the augmented Jacobian matrix. In the second part of the algorithm, an optimal nonlinear feedback is designed. In this part, the designing of the initial control law, $u^{(0)}(x)$, and choosing a proper set of basis functions are important and a critical point for convergence of the algorithm. In the third part, the DLCC of the mobile manipulator is determined using this controller, subject to accuracy and the actuator constraints.

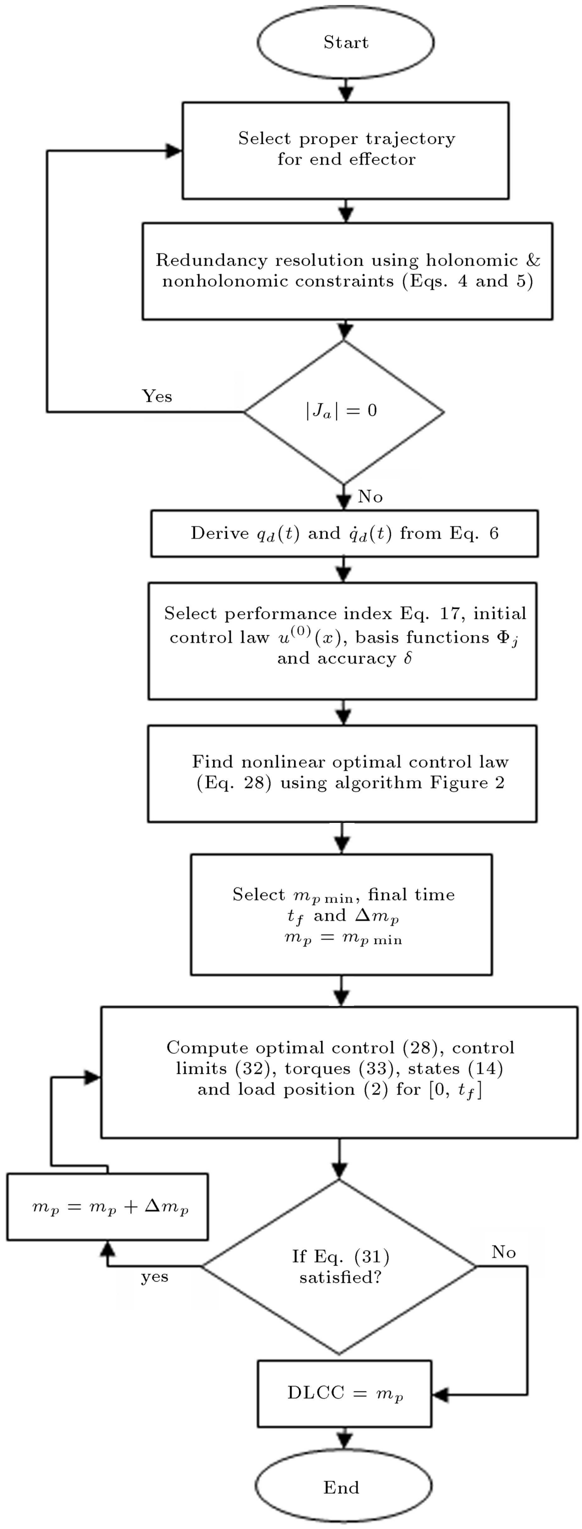

Figure 3. Algorithm for calculating DLCC.

SIMULATION RESULTS

Planar Wheeled Mobile Manipulator with Two Arms

The proposed algorithm is applied to a two-link planar manipulator that is mounted on a differentially driven mobile base to investigate the application and effectiveness of the algorithm. A schematic view of this mobile manipulator is shown in Figure 4. The parameters of the links and base and their inertia properties are given in Table 1 [6]. Generalized coordinates of the system are:

Table 1. Parameters and inertia properties of planar mobile manipulator.

Parameter	Value	Unit
Length of links	$L_1 = L_2 = 0.5$	m
Center of mass	$L_{c1} = L_{c2} = 0.25$	m
Mass of links	$m_1 = 5$, $m_2 = 3$	kg
Moment of inertia of links 1, 2	$I_1 = 0.416$, $I_2 = 0.0625$	kg.m^2
Mass of base	94	kg
Mass of wheels	5	kg
Moment of inertia of base	$\begin{bmatrix} 0 & 0 & 0 \\ 0 & 0 & 0 \\ 0 & 0 & 6.609 \end{bmatrix}$	kg.m^2
Moment of inertia of wheels	$\begin{bmatrix} 0.131 & 0 & 0 \\ 0 & 0.01 & 0 \\ 0 & 0 & 0.131 \end{bmatrix}$	kg.m^2
b	0.171	m
r	0.075	m
L_0	0.4	m

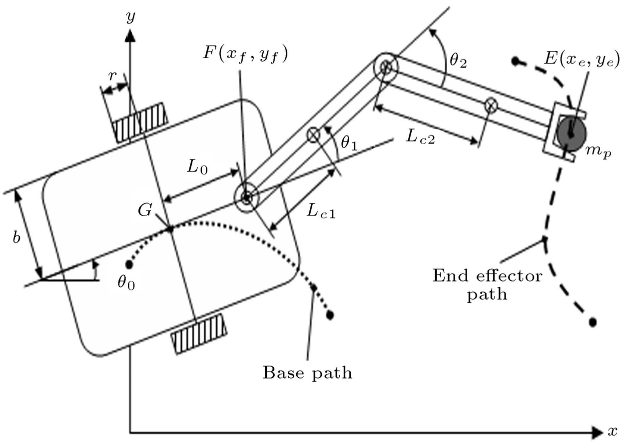

Figure 4. Schematic view of wheeled mobile manipulator.

$$q = \begin{bmatrix} q_b & q_m \end{bmatrix} = \begin{bmatrix} x_f & y_f & \theta_0 & \theta_1 & \theta_2 \end{bmatrix}, \qquad (34)$$

where $q_b = \begin{bmatrix} x_f & y_f & \theta_0 \end{bmatrix}$ are generalized coordinates describing the motion of the mobile base and $q_m = \begin{bmatrix} \theta_1 & \theta_2 \end{bmatrix}$ are the generalized coordinates of the manipulator. So, the degree of freedom of the system is equal to $n_s = 5$. As Figure 4 shows, two parameters, x_e and y_e, specify the position of the end-effector in Cartesian space, and Equation 2 can be rewritten as:

$$X = \begin{bmatrix} x_e \\ y_e \end{bmatrix} = \begin{bmatrix} x_f + L_1 \cos(\theta_0 + \theta_1) + L_2 \cos(\theta_0 + \theta_1 + \theta_2) \\ y_f + L_1 \sin(\theta_0 + \theta_1) + L_2 \sin(\theta_0 + \theta_1 + \theta_2) \end{bmatrix}. \qquad (35)$$

Thus, the degree of freedom of the end-effector is $n_e = 2$ and the order of redundancy of the system is $R = n_s - n_e = 3$, which is the number of required constraints in order to reach the redundancy resolution. The number of nonholonomic constraints of the system is $c = 1$ and is of the form:

$$\dot{x}_f \sin(\theta_0) - \dot{y}_f \cos(\theta_0) + L_0 \dot{\theta}_0 = 0. \qquad (36)$$

The cause of this constraint is the no-slippage rolling condition of the driven wheels. Hence, $r = R - c = 2$ is the number of extra kinematical constraints, which must be applied to this system for redundancy resolution. Suppose that the base trajectory is previously specified and point F moves on this trajectory during the motion, thus two additional constraints will be base position coordinates, x_f and y_f.

$$X_z = \begin{bmatrix} Z_1 \\ Z_2 \end{bmatrix} = \begin{bmatrix} x_f \\ y_f \end{bmatrix}, \qquad (37)$$

where Z_1 and Z_2 are functions of time and, by differentiating them with respect to time, $\dot{x}_f, \dot{y}_f, \ddot{x}_f$ and $\ddot{y}_f$ can also be obtained, which is used in dynamic equations of the manipulator and, then the angular position and velocity of the base can be determined using Equation 36. Using the Lagrange method, dynamic equations can be obtained as [6]:

$$\begin{bmatrix} F_x \\ F_y \\ T_0 \\ \tau_1 \\ \tau_2 \end{bmatrix} = \begin{bmatrix} J_{11} & J_{12} & J_{13} & J_{14} & J_{15} \\ J_{12} & J_{22} & J_{23} & J_{24} & J_{25} \\ J_{13} & J_{23} & J_{33} & J_{34} & J_{35} \\ J_{14} & J_{24} & J_{34} & J_{44} & J_{45} \\ J_{15} & J_{25} & J_{35} & J_{45} & J_{55} \end{bmatrix} \begin{bmatrix} \ddot{x}_f \\ \ddot{y}_f \\ \ddot{\theta}_0 \\ \ddot{\theta}_1 \\ \ddot{\theta}_2 \end{bmatrix} + \begin{bmatrix} C_1 \\ C_2 \\ C_3 \\ C_4 \\ C_5 \end{bmatrix}, \qquad (38)$$

where, J_{ij} $i,j = 1,\cdots,5$ are functions of $q = [x_f \quad y_f \quad \theta_0 \quad \theta_1 \quad \theta_2]$ and C_i $i = 1,\cdots,5$ are functions of q and $\dot{q}$. The generalized coordinates can be divided in two parts: redundant part, $q_r = [x_f \; y_f \; \theta_0]$, and non-redundant part, $q_{nr} = [\theta_1 \; \theta_2]$. The two last rows of Equation 38 are associated with the non-redundant part and can be written as:

$$\begin{bmatrix} \tau_1 \\ \tau_2 \end{bmatrix} = \begin{bmatrix} J_{44} & J_{45} \\ J_{45} & J_{55} \end{bmatrix} \begin{bmatrix} \ddot{\theta}_1 \\ \ddot{\theta}_2 \end{bmatrix} + \begin{bmatrix} R_1 \\ R_2 \end{bmatrix}. \qquad (39)$$

In this equation, τ_1 and τ_2 are motor torques in joints, and coefficients R_1 and R_2 are:

$$R_1 = J_{14}\ddot{x}_f + J_{24}\ddot{y}_f + J_{34}\ddot{\theta}_0 + C_4,$$

$$R_2 = J_{15}\ddot{x}_f + J_{25}\ddot{y}_f + J_{35}\ddot{\theta}_0 + C_5. \qquad (40)$$

In Equations 39 and 40, the redundant coordinates and their derivatives are known and all coefficients are nonlinear functions of $\theta_1, \theta_2, \dot{\theta}_1$ and $\dot{\theta}_2$. Non-redundant coordinates and their derivatives are selected as state space variables as:

$$X_1 = \begin{bmatrix} \theta_1(t) \\ \theta_2(t) \end{bmatrix} = \begin{bmatrix} x_1(t) \\ x_3(t) \end{bmatrix},$$

$$X_2 = \begin{bmatrix} \dot{\theta}_1(t) \\ \dot{\theta}_2(t) \end{bmatrix} = \begin{bmatrix} x_2(t) \\ x_4(t) \end{bmatrix}. \qquad (41)$$

The state space form of the dynamical equation of motion, using Equation 39, becomes:

$$\dot{x}_1 = x_2,$$

$$\dot{x}_2 = P(J_{55}(U_1 - R_1) - J_{45}(U_2 - R_2)),$$

$$\dot{x}_3 = x_4,$$

$$\dot{x}_4 = P(-J_{45}(U_1 - R_1) + J_{44}(U_2 - R_2)), \qquad (42)$$

where:

$$P = 1/(J_{44}J_{55} - J_{45}^2).$$

Simulation Conditions

The simulation is performed using the presented algorithm as shown in Figure 3. The accuracy value in the maximum load calculation is selected as $\Delta m_p = 0.01$ kg; motor parameters are considered to be $[\tau_{s1} \quad \tau_{s2}] = [34.67 \quad 12.21]$ N.m and $[\omega_{nl1} \quad \omega_{nl2}] = [5.37 \quad 5.09]$ rad/sec. Weighting matrixes in Equation 17 are $Q_{4\times4} = \text{diag}(1)$ and $R_{2\times2} = \text{diag}(1e-4)$. The iteration accuracy of the coefficients in the algorithm of Figure 2 is selected as $\delta = 1e-2$. A standard second order set of polynomial functions is chosen as the basis functions required in the algorithm of Figure 2 as below:

$$\{\phi_j\}_{j=1}^{10} = \left\{ \begin{matrix} x_1^2, x_1x_2, x_2^2, x_1x_3, x_2x_3, \\ x_3^2, x_1x_4, x_2x_4, x_3x_4, x_4^2 \end{matrix} \right\}. \qquad (43)$$

A standard LQ controller is designed as the initial stabilizing controller $u^{(0)}(x)$, via linearizing dynamic equations of motion. The domain of states variation is as follows:

$$-3\pi \text{ rad} \leq x_1 \leq +\, 3\pi \text{ rad},$$

$$-4 \text{ rad/sec} \leq x_2 \leq +\, 4 \text{ rad/sec},$$

$$0.1 \text{ rad} \leq x_3 \leq 3 \text{ rad},$$

$$-4 \text{ rad/sec} \leq x_4 \leq +\, 4 \text{ rad/sec}. \qquad (44)$$

The algorithm of Figure 3 is presented for the end-effector tracking of a 1×1 m^2 square trajectory. At the beginning of the motion, the end-effector is at the left-hand upper corner of the square and point F at the origin. According to Equation 37, the base is forced to move on a predefined trajectory. It is considered that the base moves from the origin to point $(2,0)$ and then returns to the origin. The motion happens in 12 sec and the initial configuration of the mobile manipulator is $\theta_0(0) = 0$, $\theta_1(0) = 0$ and $\theta_2(0) = 90°$. Under this condition, the maximum payload is found to be 5.04 kg. The obtained end-effector trajectories for no load and full load conditions are shown in Figure 5. This figure shows that the nonlinear optimal control has good effects for tracking the square trajectory. The configuration of the mobile manipulator with full load is demonstrated in Figure 6. The angular positions and velocities of joints are given in Figures 7 and 8, respectively. The torque of joints is shown in Figures 9 and 10.

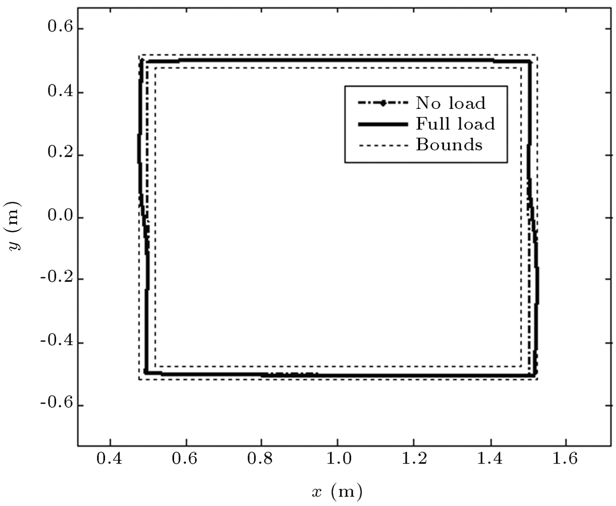

Figure 5. No load and full load trajectory.

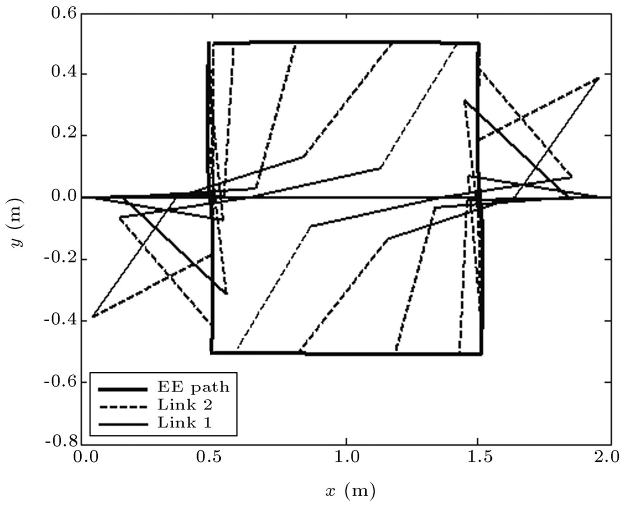

Figure 6. Configuration of mobile manipulator in motion with full load.

Linear Tracked Puma

For the second example, a spatial three-jointed Puma robot mounted on a linear tracked base is considered. A schematic view of this robot is shown in Figure 11. The manipulator characteristics and $D-H$ parameters, which are the same as used in [6] are given in Table 2. The base mass is assumed to be 21 kg. An optimal trajectory, which is designed in [6], is considered as the desired trajectory that must be tracked. The initial coordinates of the point-mass load are $E_0 = (x_e = 0.5$ m, $y_e = 0$, $z_e = -0.1$ m) and it must reach the final point with coordinates $E_f = (x_e = 0,\ y_e = 1.2$ m, $z_e = 1.04$ m$)_f$ at $t_f = 2.4$ sec through an optimal trajectory.

The generalized coordinates can be considered as $q = [x_f \quad \theta_1 \quad \theta_2 \quad \theta_3]$. The end-effector degree of freedom is $n_e = 3$ and the system degree of freedom is equal to $n_s = 4$. Consequently, the system has one degree of redundancy and needs one additional kinematical constraint for redundancy resolution. As

Table 2. Links parameters and inertia properties of Puma arm.

No.	Mass (kg)	Moment of Inertia (kg m^2)	Center of Mass (m)	$D-H$ Parameters θ_i	α_i	ai (m)	d_i (m)
1	12	$\begin{bmatrix} 0.2 & 0 & 0 \\ 0 & 0.2 & 0 \\ 0 & 0 & 0 \end{bmatrix}$	$\begin{bmatrix} 0 \\ -0.2 \\ 0 \end{bmatrix}$	θ_1	90	0	0.4
2	10	$\begin{bmatrix} 0 & 0 & 0 \\ 0 & 0.2 & 0 \\ 0 & 0 & 0.2 \end{bmatrix}$	$\begin{bmatrix} -0.25 \\ 0 \\ 0 \end{bmatrix}$	θ_2	0	0.5	0
3	5	$\begin{bmatrix} 0 & 0 & 0 \\ 0 & 0.1 & 0 \\ 0 & 0 & 0.1 \end{bmatrix}$	$\begin{bmatrix} -0.25 \\ 0 \\ 0 \end{bmatrix}$	θ_3	0	0.5	0

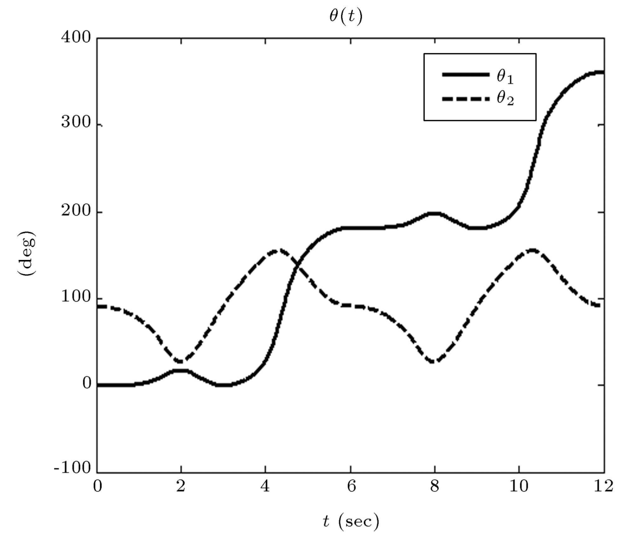

Figure 7. Angular positions of joints.

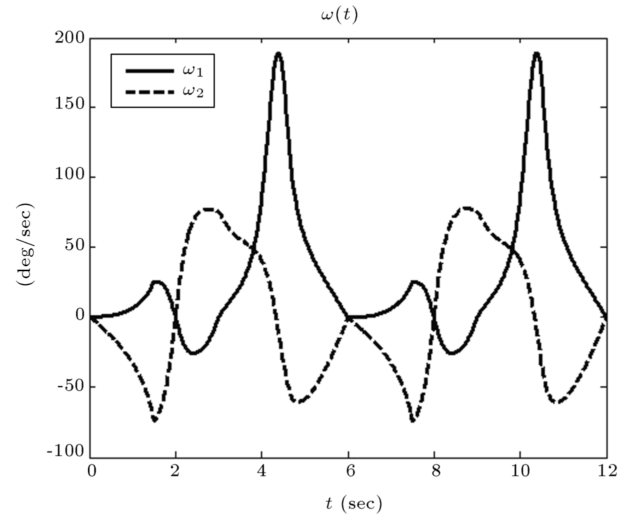

Figure 8. Angular velocities of joints.

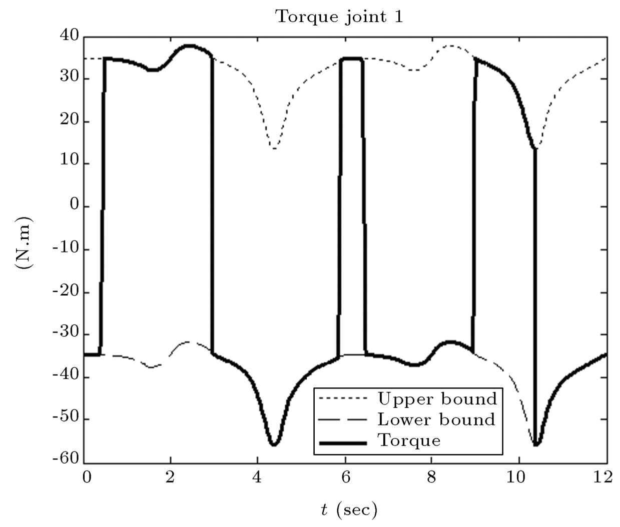

Figure 9. Actuator torque at first joint.

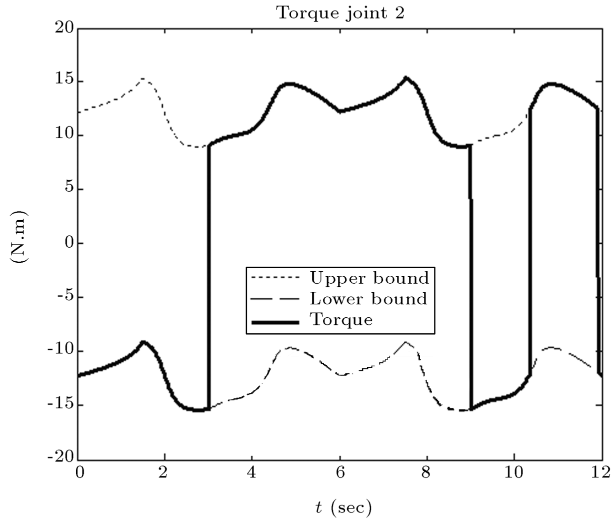

Figure 10. Actuator torque at second joint.

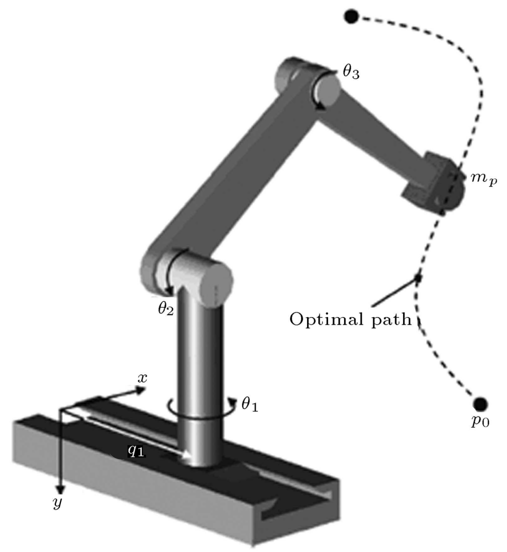

Figure 11. Puma mobile manipulator with linear tracked base.

in [6], a pre-specified fifth order polynomial function from $x_f(0) = 0$ to $x_f(t_f) = 0.347$ m is considered for the base motion. Motor parameters τ_{s1}, τ_{s2} and τ_{s3} are considered to be $[10 \quad 30 \quad 6.67]$ N.m and ω_{n11}, ω_{n12} and ω_{n13} to be $[5.71 \quad 6.41 \quad 4.6]$ rad/sec. Matrixes in Equation 17 are $Q_{6\times 6} = \mathrm{diag}(1)$ and $R_{3\times 3} = \mathrm{diag}(1e-3)$. Also, the tracking accuracy is selected as $\alpha = 0.002$ m. The required basis functions are selected as below:

$$\{\phi_j\}_{j=1}^{21} = \left\{\begin{matrix} x_1^2, x_1x_2, x_1x_3, x_1x_4, x_1x_5, x_1x_6, \\ x_2^2, x_2x_3, x_2x_4, x_2x_5, x_2x_6, x_3^2, \\ x_3x_4, x_3x_5, x_3x_6, x_4^2, x_4x_5, \\ x_4x_6, x_5^2, x_5x_6, x_6^2 \end{matrix}\right\}. \tag{45}$$

For this value of α, the maximum payload is found to be 12.03 kg. Figure 12 shows the desired and actual

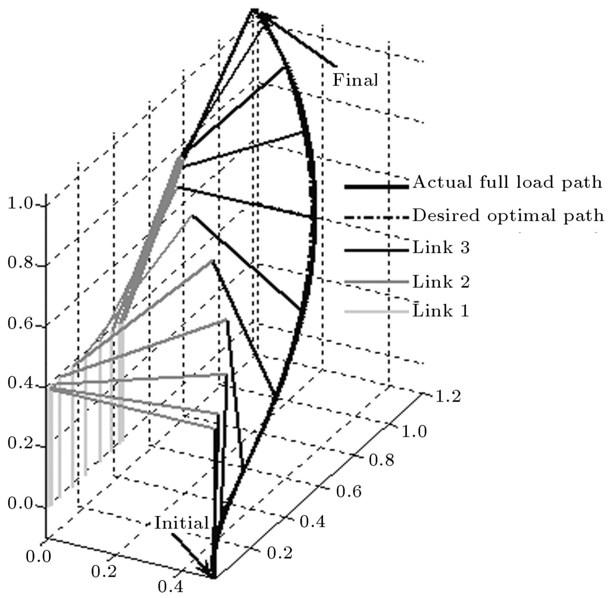

Figure 12. Actual and desired path of end-effector.

trajectory of the end-effector and the configuration of links in Cartesian space. Figures 13 to 16 illustrate the tracking error and the torque of joints 1, 2 and 3, respectively. The angular position and velocity of the joints are given in Figures 17 to 22.

CONCLUSION

In this paper, the Dynamic Load Carrying Capacity (DLCC) of a two link manipulator mounted on wheeled mobile base, and a spatial three-jointed Puma robot mounted on a linear tracked base, which are redundant systems, is determined using a nonlinear optimal feedback controller. A new algorithm is presented to investigate the application of this controller to determine the DLCC of mobile manipulators for a

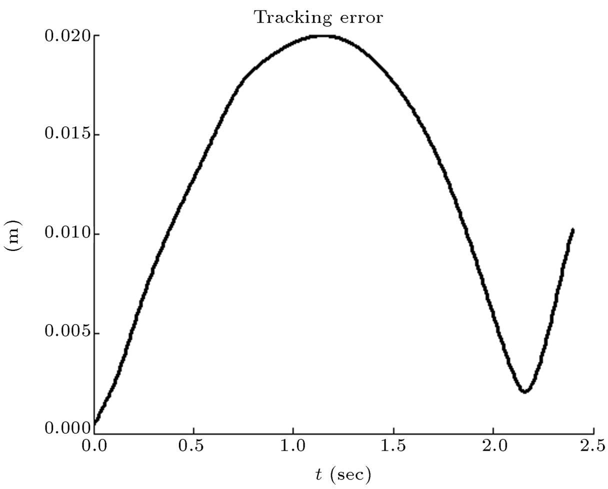

Figure 13. Error between desired optimal path and actual path .

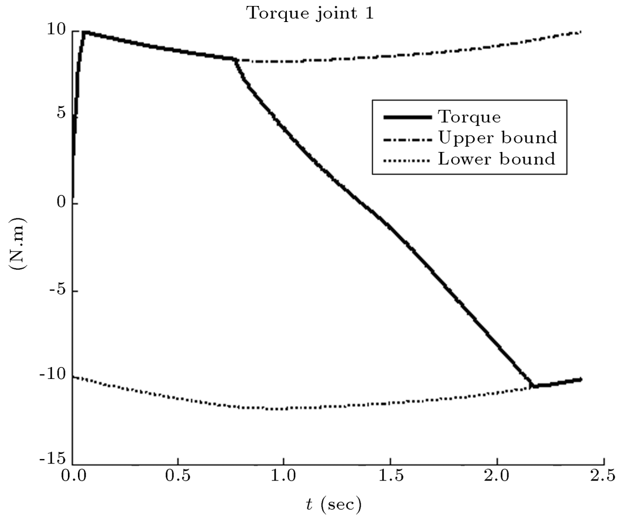

Figure 14. Torques of joint 1.

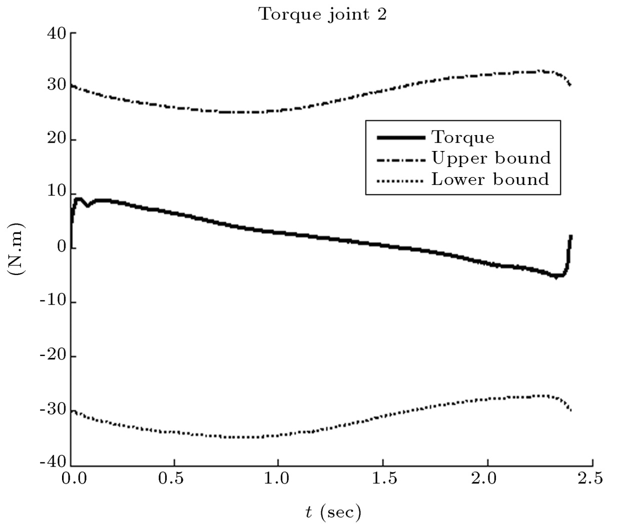

Figure 15. Torques of joint 2.

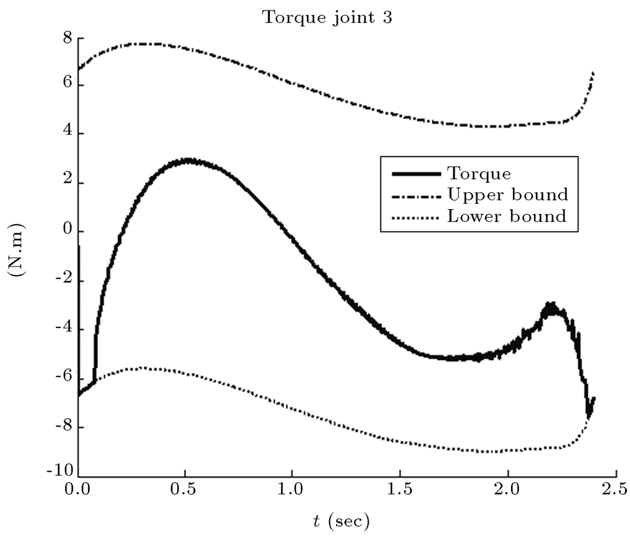

Figure 16. Torques of joint 3.

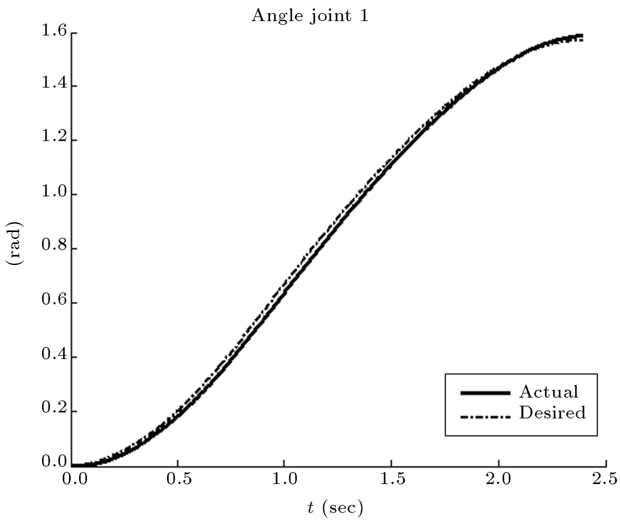

Figure 17. Angular position of joint 1.

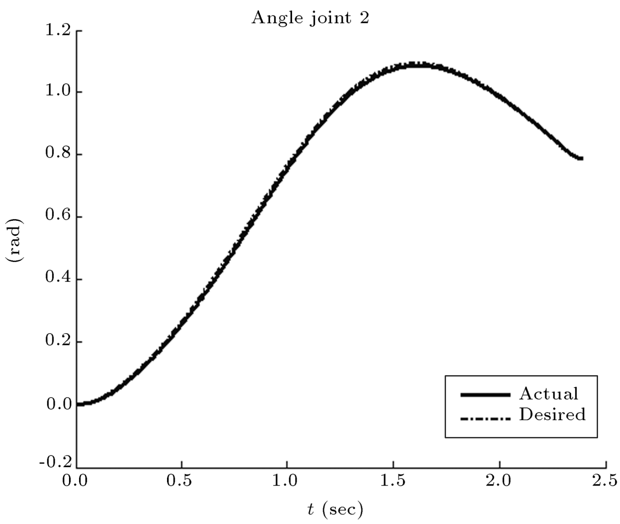

Figure 18. Angular position of joint 2.

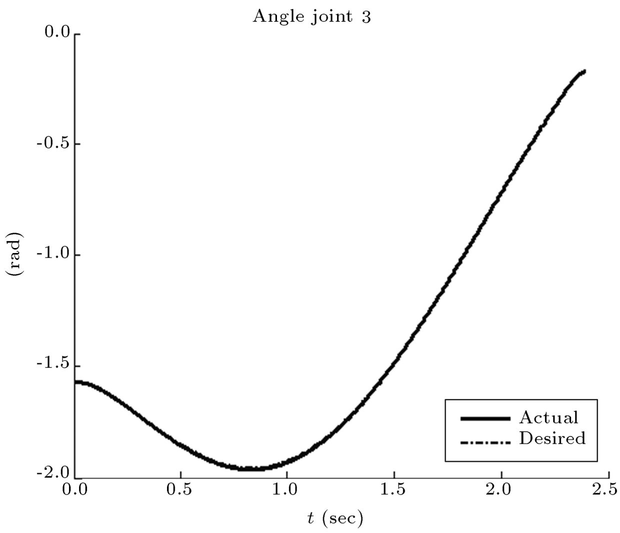

Figure 19. Angular position of joint 3.

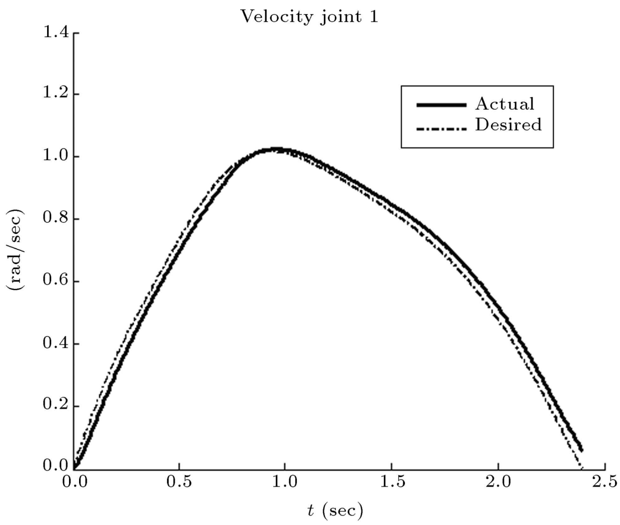

Figure 20. Angular velocity of joint 1.

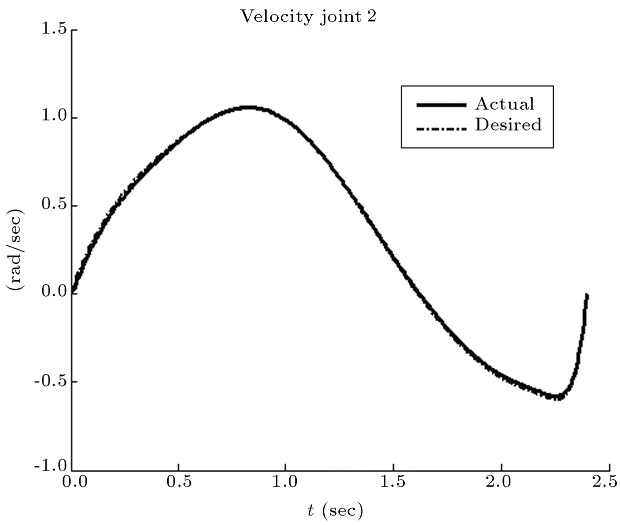

Figure 21. Angular velocity of joint 2.

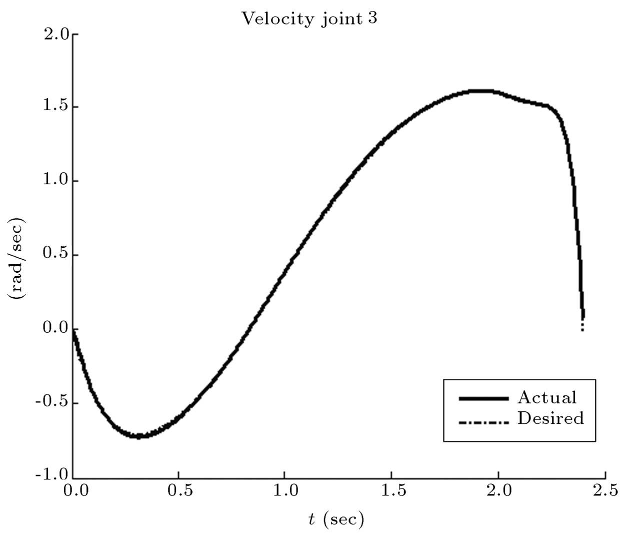

Figure 22. Angular velocity of joint 3.

given trajectory. Proper constraints are applied to the system for redundancy resolution and an augmented Jacobian matrix is derived to describe the relation between the joint space and the task space that is used in the algorithm for determining the DLCC. For designing an optimal controller, the Hamilton-Jacobi-Bellman equation is solved using an applicable algorithm based on successive approximation and the Galerkin approach. A LQ controller is selected as an initial stabilizing controller that must be used at the beginning of the algorithm. Fully nonlinear dynamic equations are used in the control design procedure. The proposed algorithm does not require solving a two point boundary value problem or linear programming, and because the control law is designed off-line and the structure of the controller is closed loop, this method is applicable and appropriate for implementation.

NOMENCLATURE

n_s	Dofs of system
n_b	Dofs of mobile platform
b	the distance between driving wheels and axis of symmetry
F	base and arm connecting point
L_0	the distance from to G to F
n	number of state variables
$\theta_1, \theta_2, \theta_3$	the angular displacements of links
τ_1, τ_2, τ_3	the torques exerted to joints
θ_0	the heading angle of platform measured from X-axis of the world coordinates
q_m	the vector of the manipulator coordinates
r	number of additional holonomic constraints
$Z(q)$	additional kinematic constraints
m_1, m_2, m_3	the mass of links
J	Jacobian matrix
J_c, J_z	matrixes appear in kinematic equations
r, nr	subscript for redundant and non-redundant variables, respectively
$G(q)$	vector of gravity force
u	input vector
$J(x)$	cost function
J^*, u^*	optimal values of J, u
c_i	Galerkin coefficient
ε	successive algorithm accuracy
α	tracking accuracy
$u^{(0)}(x)$	initial stabilizing controller
Δm_p	variations of m_p in maximum load calculation algorithm
t_f	final time
ω_{nl}	maximum no-load speed of motors
n_e	Dofs of end-effector
n_m	Dofs of links
G	the intersection of the axis of symmetry with the driving wheel axis
E	end-effector position
r	the radius of wheels
m	number of control variables
(x_f, y_f)	the coordination of F
$X = (x_e, y_e, z_e)$	the coordination of E
q	the vector of generalized coordinates of the system
q_b	the vector of mobile base coordinates
c	number of nonholonomic constraints
l_1, l_2, l_3	the length of links
m_p	the mass of payload
J_a	augmented Jacobian matrix
$M(q)$	$n_s \times n_s$ inertial matrix
$C(q.\dot{q})$	vector of Coriolis and centrifugal forces
x	vector of state variables
N, Z, f, g	nonlinear terms in state space equations
Q, R	states and control weighting matrixes
N	number of basis functions
$\phi_i(x)$	Galerkin basis function
δ	convergence accuracy of Galerkin coefficients
$X_d(q)$	desired position of end-effector
Ω	stability region of initial controller
$m_{P\,\min}$	initial value of m_p
τ_s	stall torque of motors
$\tau_{i\,\min}, \tau_{i\,\max}$	lower and upper value of ith joint torque

REFERENCES

1. Wang, L.T. and Ravani, B. "Dynamic load carrying capacity of mechanical manipulators-Part 1", *J. Dyn. Syst. Meas. Control*, **110**(1), pp. 46-52 (1988).
2. Wang, C.Y.E., Timoszyk, W.K. and Bobrow, J.E. "Payload maximization for open chained manipulators: Finding weightlifting motions for a Puma 762 robot", *IEEE Transactions on Robotics and Automation*, **17**(2), pp. 218-224 (2001).
3. Korayem, M.H., Ghariblu, H. and Basu, A. "Maximum allowable load of mobile manipulator for two given end points of end-effector", *Int. J. of AMT*, **24**(10), pp. 743-751 (2004).

4. Korayem, M.H. and Ghariblu, H. "Maximum allowable load on wheeled mobile manipulators imposing redundancy constraints", *Robotics and Autonomous Systems*, **44**(2), pp. 151-159 (2003).

5. Xu, D., Hu, H., Calderon, C.A.A. and Tan, M. "Motion planning for a mobile manipulator with redundant DOFs", *Proc ICIC'05 Conf. Intelligent Computing*, china, pp. 23-26 (2005)

6. Korayem, M.H., Nikoobin, A. and Azimirad, V. " Maximum load carrying capacity of mobile manipulators: optimal control approach", *Robotica*, **27**(1), pp. 147-159 (2009).

7. Korayem, M.H. and Nikoobin, A. "Formulation and numerical solution of robot manipulators in point-to-point motion with maximum load carrying capacity", *Scientia Iranica, Trans. B*, **16**(1), pp. 101-109 (2009).

8. Kelly, A. and Nagy, B. "Reactive nonholonomic trajectory generation via parametric optimal control", *Int. J. of Robotics Research*, **22**(8), pp. 583-601 (2003).

9. Furuno, S., Yamamoto, M. and Mohri, A. "Trajectory planning of mobile manipulator with stability considerations", *IEEE Int. Conf. on Robotics & Automation*, Taipei, Taiwan, pp. 3403-3408 (2003).

10. Dos Santos, R.R., Steffen, V. and Saramago, S.F.P. "Robot path planning in a constrained workspace by using optimal control techniques", *Multibody Syst. Dyn.*, **19**(2), pp. 159-177 (2008).

11. Korayem, M.H. and Shokri, M. "Maximum dynamic load carrying capacity of a 6UPS-Stewart platform manipulator", *Scientia Iranica*, **15**(1), pp. 131-143 (2008).

12. Van Willigenburg, L.G., De Koning, W.L., Chalabi, Z.S. and Tchamitchian, M. "On the selection of appropriate control system design methodologies", *IFAC World Congress*, Prague (2005).

13. Papadopoulos, E. and Poulakakis, J. "Trajectory planning and control for mobile manipulator systems", *8th IEEE Conf. on Control & Automation*, Rio, Greece (2000).

14. Song, Z., Zhao, D., Yi, J. and Li, X. "Tracking control of mobile manipulator with dynamical uncertainties", *IEEE Int. Conf. on Intelligent Robots and Systems*, pp. 759-764 (2005).

15. Reyes, F. and Rosado, A. "Polynomial family of PD-type controllers for robot manipulators", *Control Engineering Practice*, **13**(4), pp. 441-450 (2005).

16. Mailah, M., Pitowarno, E. and Jamaluddin, H. "Robust motion control for mobile manipulator using resolved acceleration and proportional-integral active force control", *Int. J. of Advanced Robotic Systems*, **2**(2), pp. 125-134 (2005).

17. Ha, T.J., Lee, J. and Park, J.H. "Robust control by inverse optimal PID approach for flexible joint robot manipulator", *IEEE Int. Conf. on Robotics and Biomimetics*, Sanya, China, pp. 336-341 (2007).

18. Abdessemed, F., Monacelli, E. and Benmahammed, K. "A new approach for mobile manipulator motion control", *8th IEEE Int. Conf. on Electronics, Circuits and Systems*, **3**, Malta, pp. 1203-1207 (2001).

19. Tran, T.P., Chung, T.L., Kim, H.K., Kim, S.B. and Oh, M.S. "Trajectory tracking of mobile manipulator for welding task using sliding mode control", *30th Annual Conf. of IEEE Industrial Electronics Society*, **1**, pp. 407-412 (2004).

20. Korayem, M.H., Firouzy, S. and Heidari, A. "Dynamic load carrying capacity of mobile-base flexible-link manipulators: feedback linearization control approach", *IEEE Int. Conf. on Robotics and Biomimetics*, pp. 2172-2177 (2007).

21. Korayem, M.H., Haghighi, R., Nikoobin, A. Alamdari, A. and Korayem, A.H. "Determining maximum load carrying capacity of flexible link manipulators", *Scientia Iranica* (article in press).

22. Green, A. and Sasiadek, J.Z. "Dynamics and trajectory tracking control of a two-link robot manipulator", *J. of Vibration and Control*, **10**(10), pp. 1415-1440 (2004).

23. Miksch, W. and Schroeder, D. "Performance-functional based controller design for a mobile manipulator", *IEEE Int. Conf. on Robotics and Automation*, Nice, France, pp. 227-232 (1992).

24. Kirk, D.E., *Optimal Control Theory*, Prentice-Hall Inc. (1970).

25. Beeler, S.C., Tran, H.T. and Banks, H.T. "Feedback control methodologies for nonlinear systems", *Journal of Optimization Theory and Applications*, **107**(1), pp. 1-33 (2000).

26. Chen, W.H., Ballance, D.J. and Gawthrop, P.J. "Optimal control of nonlinear systems: a predictive control approach", *Automatica*, **39**(4), pp. 633-641 (2003).

27. Sjoberg, J. and Glad, T. "Power series solution of the Hamilton-Jacobi-Bellman equation for time-varying differential-algebraic equations", *45th IEEE Conf. on Decision & Control*, San Diego, USA, pp. 870-875 (2006).

28. Cimen, T. "State-Dependent Riccati equation (SDRE) control: a survey", *17th World Congress of the Int. Fed. of Automatic Control*, Seoul, Korea, pp. 3761-3775 (2008).

29. Xin, M., Balakrishnan, S.N. and Huang, Z. "Robust state dependent Riccati equation based robot manipulator control", *IEEE Int. Conf. on Control Applications*, Mexico City, Mexico, pp. 369-374 (2001).

30. Beard, R.W. and McLain, T.W. "Successive Galerkin approximation algorithms for nonlinear optimal and robust control", *Int. J. of Control*, **71**(5), pp. 717-743 (1998).

BIOGRAPHIES

M. Habibnejad Korayem was born in Tehran, Iran, on April 21st, 1961. He received his BS (Hon) and MS in mechanical engineering from Amirkabir University of Technology in 1985 and 1987, respectively. He obtained his PhD degree in mechanical engineering from the University of Wollongong, Australia, in 1994, and is now a professor of mechanical engineering at the Iran University of Science and Technology, where, for the last 15 years, he has been involved in teaching and research activities in the area of robotics. His research interests include; dynamics of elastic mechanical manipulators, trajectory optimization, symbolic modeling, robotic multimedia software, mobile robots, industrial robotics standard, robot vision, soccer robots, and the analysis of mechanical manipulators with maximum load carrying capacity. He has published more than 300 papers in international journals and conference publications in the area of robotics.

M. Irani was born in Kashan, Iran on 22nd July, 1980. He received his BS in mechanical engineering from Isfahan University of Technology in 2002 and a MS in aerospace engineering from the KNTU University of Technology in 2005. Since 2007, he has been pursuing his PhD degree course in mechanical engineering at the Iran University of Science and Technology. His research interests include; robotic systems, nonlinear control, optimal control, mobile manipulators, industrial automation and mechatronic systems.